Measurements of the aerosol single scattering albedo in the UV over Thessaloniki, Greece

Fountoulakis I.[1*], Natsis A.[1], Siomos N. [1], Drosoglou T. [1], Bais A. [1], Balis D. [1], Kazadzis S. [2,3]

1 Laboratory of atmospheric physics, Physics Department, Aristotle University of Thessaloniki, Greece.

2 Physikalisch-Meteorologisches Observatorium Davos, World Radiation Center (PMOD/WRC), Dorfstrasse 33, 7260 Davos Dorf, Switzerland

3 Institute of Environmental Research and Sustainable Development, National Observatory of Athens, Greece

*corresponding author e-mail: iliasnf@auth.gr

Abstract At the facilities of the Laboratory of Atmospheric Physics of the Aristotle University of Thessaloniki, Greece, a double monochromator Brewer spectrophotometer records nearly simultaneous direct and global solar UV irradiance spectral measurements at 10 nm intervals between 310 and 360 nm. At these wavelengths, the effective single scattering albedo (SSA) of aerosols is calculated by comparing the ratio between the direct and global irradiance with the corresponding ratio from simulations by a radiative transfer model, for the same atmospheric conditions. A comprehensive uncertainty analysis has been performed regarding the calculation of the SSA in this spectral region, which shows that two important uncertainty factors above 320 nm are the measured irradiance levels and the AOD, while below 320 nm the total ozone is also an important factor of uncertainty. The effect of using default aerosol extinction profiles in the simulations, instead of the real ones, has been also investigated for specific cases using lidar profiles. Comparison with measurements of the SSA in the visible spectral region from a co-located CIMEL sun-photometer shows that the SSA in the UV is significantly lower confirming the findings of other recent studies.

1 Introduction

Although numerous studies are focused on explaining the physical and chemical processes in the atmosphere affected by aerosols (IPCC, 2013), and have shed light in the complicated interactions between aerosols and solar radiation, (e.g. Kazadzis et al. (2009)), the level of understanding remains low. The description of the role of aerosols in global climate models and satellite algorithms is still poor, making aerosols a major uncertainty factor in both, model simulations and satellite retrievals (Lee et al., 2016; Samset et al., 2013).

The understanding of the interactions between aerosols and solar radiation in the UV region is even lower compared to the visible part of the solar spectrum (e.g. Palancar et al. (2013)). Although measurements of the aerosol optical depth (AOD) in the UV are nowadays available by large networks (Holben et al., 1998; Nakajima et al., 1996), providing useful information regarding the specific parameter, very few stations provide reliable measurements of the absorption efficiency of aerosols in UV, usually described by the single scattering albedo (SSA) and the absorption optical depth (AAOD).

Several studies suggest that, for particular aerosol species, the SSA in the UV differs largely from the corresponding SSA in the visible region, (e.g. Corr et al. (2009)), pointing out the need for reliable measurements of SSA in UV, also given the vital importance of UV radiation for humans and the ecosystems. In the present study, the methodology described by (Bais et al., 2005) has been used to calculate and study the SSA over Thessaloniki in the spectral region 310 – 360 nm with a step of 10 nm. Analysis of the uncertainties in the calculation of the SSA has been also performed.

2 Data and Methodology

For the calculation of the SSA, direct-sun and global UV measurements from the double monochromator Brewer (type MKIII) with serial number 086 (Brewer#086) have been used. The particular instrument is operating at the facilities of the Laboratory of Atmospheric Physics of the Aristotle University of Thessaloniki, Greece (LAP) since 1993, and performs automated measurements of the global solar irradiance in the region 290 – 363 nm with a step and a resolution of 0.5 nm. The temporal resolution of the spectral scans is ~ 20 – 30 mins. Since 1997, each spectral scan of the global UV irradiance is interrupted at specific wavelengths (300 – 360 nm with a step of 10 nm) and measurements of the direct sun irradiance are performed. The temporal difference between the measurements of the direct sun irradiance and the corresponding measurements of the global irradiance at the same wavelength is of the order of a few seconds, thus they are considered simultaneous. The ratio of the direct and global irradiance is then calculated and used for the retrieval of the SSA.

For each of these measurements, simulations are performed with the radiative transfer model (RTM) uvspec, of the libRadtran package, version 2.0 (Emde et al., 2016), for the same AOD, total ozone, and solar zenith angle and different values of the SSA (from 0.3 to 1 with a step 0.01). The direct to global irradiance ratio from Brewer#086 is then compared with the corresponding modeled ratios and the SSA is considered to be that, for which the modeled ratio is closest to the measured one. The AOD used in the RTM is directly calculated from the same direct irradiance measurements used for the calculation of the ratio (Kazadzis et al., 2005). The total ozone is derived from a single monochromator MKII Brewer with serial number 005 (Brewer#005), also operating at the facilities of LAP. The closest to the direct-to-global irradiance ratio total ozone measurement is used in the model. If no measurements of total ozone are available for a particular day, this day is discarded. Cloud screening of the measured ratios is achieved using data from a CM-21 pyranometer (Vasaras et al., 2001) and only ratios measured under cloudless skies are used in the analysis. The SSA at 340 nm has been also calculated using the 340 nm (level 1.5) AOD product from a co-located CIMEL sun-photometer as input to the RTM. The level 1.5 SSA product at 440 nm from CIMEL has been compared with the SSA from Brewer#086. Simulations have been also performed using extinction coefficient profiles from the lidar also operating at LAP, to quantify the effect of using a default aerosol profile.

3 Results

In the present study the SSA in the UV (310 – 360 nm) derived from Brewer#086 is presented for the year 2015, and compared to the SSA in the visible region (440 nm) as it is calculated from measurements performed by CIMEL sun-photometer. Furthermore, an effort is made to quantify the main uncertainties in the calculation of the SSA from the Brewer.

3.1 Uncertainties

According to Kazadzis et al. (2016), the main factors introducing uncertainties in the measurements of Brewer#086 are:

- Uncertainties in the AOD used for the RTM simulations
- Uncertainties in the AOD and SSA profiles used for the RTM simulations
- Uncertainties in the profile and the total column of ozone (important for UV-B wavelengths)
- Calibration uncertainties
- Measurement uncertainties

The 1-sigma uncertainties in the retrieval of the (extinction) AOD from Brewer#086 have been estimated to 0.05 for UV-A and 0.07 for UV-B (Kazadzis et al., 2007). Comparison between measurements by Brewer and CIMEL confirms their findings since the mean difference between the level 1.5 AOD at 340 nm from the two instruments (for the year 2015) is 0.01 ± 0.03. The (absolute and relative) difference between the calculated SSA, when the AOD from the Brewer or the CIMEL are used in the simulations, is shown in Figure 1.

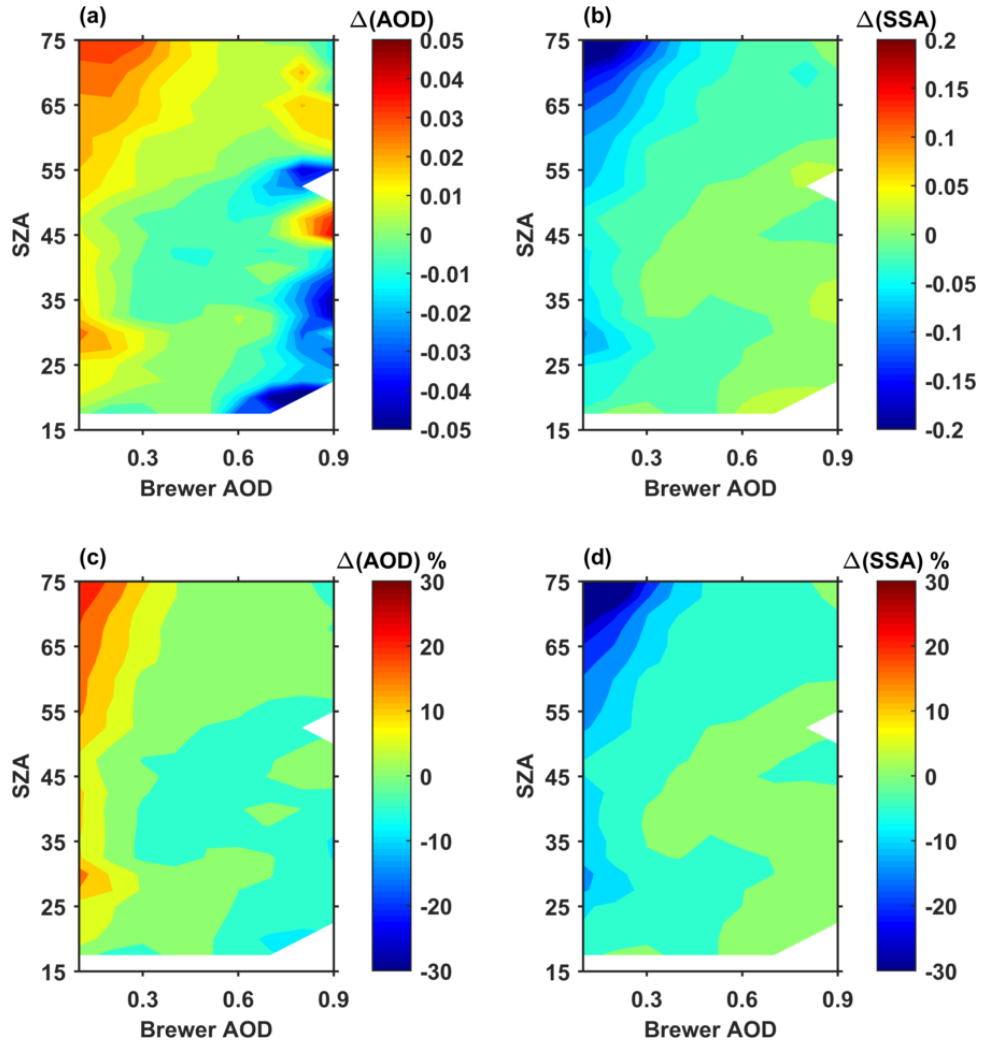

Fig. 1. (a) Absolute differences between the AOD from Brewer and CIMEL at 340 nm (for 2015), **(b)** absolute differences between the SSA at 340 nm when AOD from the Brewer and CIMEL is used in the simulations, **(c)** same as (a) showing the relative (%) instead of the absolute differences, and **(d)** same as (b) showing the relative (%) instead of the absolute differences,.

From Figures 1a and 1c it is evident that the Brewer usually reports higher AOD (by up to ~0.035), particularly when the AOD is low. The impact of this overestimation in the calculation of the SSA also becomes more important for lower AOD values (Figures 1b and 1c), for which the relative differences between the AOD from the two instruments are larger (Figure 1c). The largest (absolute and relative) differences in AOD occur at high SZA, inducing correspondingly large differences in the SSA.

Different extinction coefficient profiles were used instead of the default aerosol profile to estimate the effect of using a climatological profile. The profiles were for six different days during which the mixture of aerosols was mainly consisted by one of the following aerosol types: dust (two days), biomass burning

(two days) and continental (two days). The profiles and the aerosol type were derived by lidar measurements (Giannakaki et al., 2010; Siomos et al., 2017). The lidar profiles have been derived at 355 nm and have been scaled to the measured AOD for the particular days. In all cases, the derived SSA is not changing by more than 0.03 for all wavelengths (310 – 360 nm). Although uncertainties due to the use of a default SSA profile in the simulations are expected to be more important, presently, there are no reliable SSA profiles which can be used to assess this effect.

Overall uncertainties in total ozone column (due to uncertainties in the used cross sections, stratospheric temperature variations, calibration and measurement uncertainties) are estimated to be of the order of ~2.3% (Carlund et al., 2017). The change of the calculated SSA due to a change of 2.3% in the total ozone column used in the simulations, is in all cases lower than 0.01 (thus not detectable). However, a 2.3% error in total ozone induces an error of 0.02 to 0.03 in the AOD calculation at 310 nm, which in turn induces a corresponding error in the calculation of the SSA, ranging from ~0 for high AOD (near 0.9) to ~0.1 for low AOD (near 0.1). Uncertainties also arise from the use of default ozone profile in the simulations, though they have not been investigated yet.

The uncertainties of the Brewer global UV irradiance calibration are not affecting the calculation of the SSA since the same calibration factor affects both terms of the ratio (direct and global irradiance). Thus, only the uncertainties in the calibration transfer function from global to direct irradiance affect the calculation of the SSA. These uncertainties have been estimated to ~3% (Kazadzis et al., 2005). For high AOD (> 0.3), changes in the ratio, of the order of 3%, have small impact in the calculation of the SSA (<0.05). Though, for low AOD the error in the calculation of the SSA becomes more important, reaching 0.3 for AOD near 0.1. Uncertainties in the measurements of the direct and global irradiance are estimated to be smaller and less significant compared to the uncertainties discussed above.

3.2 Annual variability of the SSA from Brewer#086 and CIMEL

In Figure 2(a), the monthly mean values of the SSA at 310, 320, 340 and 360 nm are presented. The monthly mean values have been calculated as averages of the daily mean SSA for the days of each month. The SSA for SZAs above 75° has not been taken into account in the analysis for both instruments. Shaded areas represent the standard deviation. There is a clear annual cycle while differences between different wavelengths are within the estimated uncertainties.

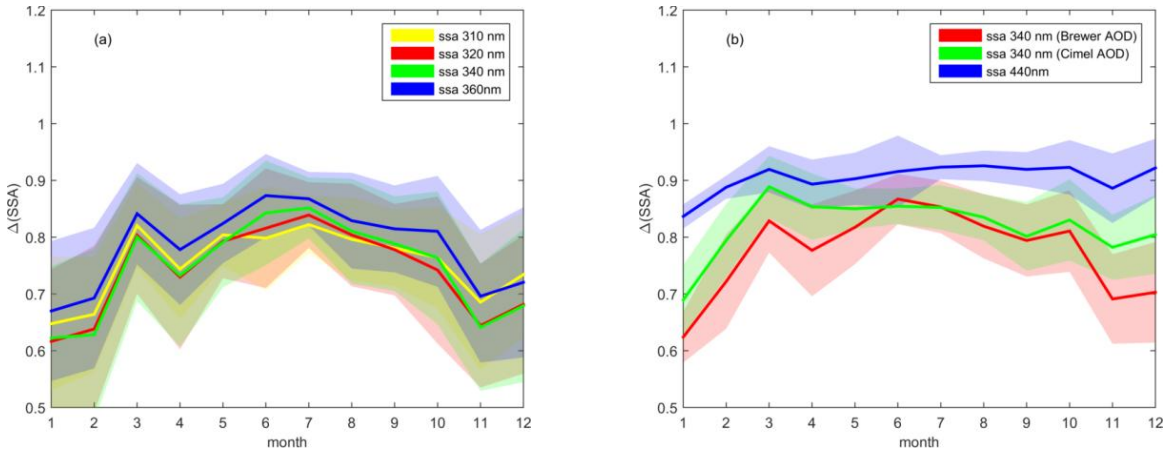

Fig. 2. (a) SSA at 310, 320, 340 and 360 nm from Brewer#086. The shaded areas represent the standard deviation and **(b)** SSA at 340 nm from Brewer#086 calculated using AOD from Brewer#86 and CIMEL and SSA at 440 nm from CIMEL.

In Figure 2(b), the monthly mean SSA at 340 nm derived from the Brewer, calculated using both the AOD derived from the Brewer and the CIMEL, and the SSA at 440 nm from the CIMEL are presented. For both cases, the SSA at 340 nm is lower than the corresponding SSA at 440 nm. When the AOD from the Brewer is used for the calculation of the SSA, the differences between the SSA at 340 and 440 nm range from ~0.05 to ~0.2, while when the AOD from the CIMEL is used in the simulations the differences become smaller, ranging from ~ 0.01 to ~ 0.15. In both cases the annual cycle of the SSA at 340 nm is more pronounced from the corresponding annual cycle of the SSA at 440 nm. During the cold period of the year the SSA at 340 nm gets very small values, possibly associated with more absorbing urban aerosols, originating mainly from local sources in this period (Amiridis et al., 2005). This behavior is not seen in the SSA at 440 nm which stay rather stable during the year with a small decrease in January. This behavior is possibly related to the smaller differences in SSA at visible than UV wavelengths for different aerosol types.

4 Conclusions

In the present study, the methodology for the retrieval of SSA in the wavelength range 310 – 360 nm from measurements performed by a double monochromator Brewer has been presented. The most important uncertainty factor in the calculation of the SSA is the magnitude of AOD. The uncertainties induced due to errors in the AOD are very important when the AOD is low (below ~0.2) and less important for higher AOD. However, the parameter that describes the radiative effect of absorption by aerosols is AAOD, which is calculated by multiplying AOD by SSA. Even large errors in SSA at low AODs induce small absolute errors in the calculation of the AAOD, thus have a small impact in the quantification of the radiative effect of the absorption by aerosols. A clear annual cycle is found for the SSA in the UV which is not evident for the SSA at 440 nm. Generally, the SSA in the UV is lower compared to the SSA at 440 nm by ~ 0.05 – 0.15 depending on month. When AOD from the CIMEL is used for the calculation of the SSA at 340 nm, the SSA values are slightly higher (compared to the SSA calculated using AOD from Brewer#086) mainly for winter. This is possibly due to the lower AOD in winter compared to the AOD during the rest of the year, which makes the differences between the AOD from the two instruments more significant, and leads to larger differences in the SSA during this period.

References

Amiridis, V., D. S. Balis, S. Kazadzis, A. Bais, E. Giannakaki, A. Papayannis, and C. Zerefos (2005), Four-year aerosol observations with a Raman lidar at Thessaloniki, Greece, in the framework of European Aerosol Research Lidar Network (EARLINET), J. Geophys. Res., 110, D21203, doi: 10.1029/2005JD006190.

Bais, A. F., Kazantzidis, A., Kazadzis, S., Balis, D. S., Zerefos, C. S., and Meleti, C.: Deriving an effective aerosol single scattering albedo from spectral surface UV irradiance measurements, Atmospheric Environment, 39, 1093-1102, http://dx.doi.org/10.1016/j.atmosenv.2004.09.080, 2005.

Carlund, T., Kouremeti, N., Kazadzis, S., and Grobner, J.: Aerosol optical depth determination in the UV using a four-channel precision filter radiometer, tmos. Meas. Tech., 10, 905 - 923, 10.5194/amt-10-905-2017, 2017.

Corr, C. A., Krotkov, N., Madronich, S., Slusser, J. R., Holben, B., Gao, W., Flynn, J., Lefer, B., and Kreidenweis, S. M.: Retrieval of aerosol single scattering albedo at ultraviolet wavelengths at the T1 site during MILAGRO, Atmos. Chem. Phys., 9, 5813-5827, 10.5194/acp-9-5813-2009, 2009.

Emde, C., Buras-Schnell, R., Kylling, A., Mayer, B., Gasteiger, J., Hamann, U., Kylling, J., Richter, B., Pause, C., Dowling, T., and Bugliaro, L.: The libRadtran software package for radiative transfer calculations (version 2.0.1), Geosci. Model Dev., 9, 1647-1672, 10.5194/gmd-9-1647-2016, 2016.

Giannakaki, E., Balis, D. S., Amiridis, V., and Zerefos, C.: Optical properties of different aerosol types: seven years of combined Raman-elastic backscatter lidar measurements in Thessaloniki, Greece, Atmos. Meas. Tech., 3, 569-578, 10.5194/amt-3-569-2010, 2010.

Holben, B. N., Eck, T. F., Slutsker, I., Tanré, D., Buis, J. P., Setzer, A., Vermote, E., Reagan, J. A., Kaufman, Y. J., Nakajima, T., Lavenu, F., Jankowiak, I., and Smirnov, A.: AERONET—A Federated Instrument Network and Data Archive for Aerosol Characterization, Remote Sensing of Environment, 66, 1-16, http://dx.doi.org/10.1016/S0034-4257(98)00031-5, 1998.

IPCC: Climate Change 2013: The Physical Science Basis. Contribution of Working Group I to the Fifth Assessment Report of the Intergovernmental Panel on Climate Change Cambridge University Press, Cambridge, United Kingdom and New York, NY, USA, 1535 pp., 2013.

Kazadzis, S., Bais, A., Kouremeti, N., Gerasopoulos, E., Garane, K., Blumthaler, M., Schallhart, B., and Cede, A.: Direct spectral measurements with a Brewer spectroradiometer: absolute calibration and aerosol optical depth retrieval, Applied Optics, 44, 1681-1690, 10.1364/ao.44.001681, 2005.

Kazadzis, S., Bais, A., Amiridis, V., Balis, D., Meleti, C., Kouremeti, N., Zerefos, C. S., Rapsomanikis, S., Petrakakis, M., Kelesis, A., Tzoumaka, P., and Kelektsoglou, K.: Nine years of UV aerosol optical depth measurements at Thessaloniki, Greece, Atmos. Chem. Phys., 7, 2091-2101, 10.5194/acp-7-2091-2007, 2007.

Kazadzis, S., Kouremeti, N., Bais, A., Kazantzidis, A., and Meleti, C.: Aerosol forcing efficiency in the UVA region from spectral solar irradiance measurements at an urban environment, Ann. Geophys., 27, 2515-2522, 10.5194/angeo-27-2515-2009, 2009.

Kazadzis, S., Raptis, P., Kouremeti, N., Amiridis, V., Arola, A., Gerasopoulos, E., and Schuster, G. L.: Aerosol absorption retrieval at ultraviolet wavelengths in a complex environment, Atmos. Meas. Tech., 9, 5997-6011, 10.5194/amt-9-5997-2016, 2016.

Lee, L. A., Reddington, C. L., and Carslaw, K. S.: On the relationship between aerosol model uncertainty and radiative forcing uncertainty, Proceedings of the National Academy of Sciences, 113, 5820-5827, 10.1073/pnas.1507050113, 2016.

Nakajima, T., Tonna, G., Rao, R., Boi, P., Kaufman, Y., and Holben, B.: Use of sky brightness measurements from ground for remote sensing of particulate polydispersions, Applied Optics, 35, 2672-2686, 10.1364/ao.35.002672, 1996.

Palancar, G. G., Lefer, B. L., Hall, S. R., Shaw, W. J., Corr, C. A., Herndon, S. C., Slusser, J. R., and Madronich, S.: Effect of aerosols and NO₂ concentration on ultraviolet actinic flux near Mexico City during MILAGRO: measurements and model calculations, Atmos. Chem. Phys., 13, 1011-1022, 10.5194/acp-13-1011-2013, 2013.

Samset, B. H., Myhre, G., Schulz, M., Balkanski, Y., Bauer, S., Berntsen, T. K., Bian, H., Bellouin, N., Diehl, T., Easter, R. C., Ghan, S. J., Iversen, T., Kinne, S., Kirkevåg, A., Lamarque, J. F., Lin, G., Liu, X., Penner, J. E., Seland, Ø., Skeie, R. B., Stier, P., Takemura, T., Tsigaridis, K., and Zhang, K.: Black carbon vertical profiles strongly affect its radiative forcing uncertainty, Atmos. Chem. Phys., 13, 2423-2434, 10.5194/acp-13-2423-2013, 2013.

Siomos, N., Balis, D. S., Poupkou, A., Liora, N., Dimopoulos, S., Melas, D., Giannakaki, E., Filioglou, M., Basart, S., and Chaikovsky, A.: Investigating the quality of modeled aerosol profiles based on combined lidar and sunphotometer data, Atmos. Chem. Phys., 17, 7003-7023, https://doi.org/10.5194/acp-17-7003-2017, 2017.

Vasaras, A., Bais, A. F., Feister, U., and Zerefos, C. S.: Comparison of two methods for cloud flagging of spectral UV measurements, Atmospheric Research, 57, 31-42, https://doi.org/10.1016/S0169-8095(00)00070-3, 2001.